Journal of Low Temperature Physics, Vol. 110, Nos. 1/2, 1998

Superfluidity of Pure ^{3}He and Mixtures of ^{3}He and ^{4}He in Aerogel

A. Golov, J. V. Porto, K. Matsumoto, L. Pollack, E. N. Smith, R. D. Biggar, T. L. Ho, and J. M. Parpia

Laboratory of Atomic & Solid State Physics
Cornell University, Ithaca, NY 14853, USA

We describe new torsional oscillator experiments on ^{3}He confined in 98.2% open aerogel. In one, we monitored the superfluid fraction of pure ^{3}He at $T << T_c$ while we gradually changed the sample pressure. The resulting change in density alters ξ_0 of the superfluid ^{3}He relative to the distribution of the length scales (correlations) of silica in the aerogel. We observed a $T = 0$ normal-to-superfluid transition at a pressure of about 6.5 bar, in marked contrast to the bulk where liquid ^{3}He is superfluid at all pressures. In the second experiment, we measured the temperature dependence of the ^{3}He ρ_s at a pressure of 21.6 bar with different amounts of ^{4}He present in the cell. Adding 2-3% ^{4}He slightly increases both T_c and ρ_s. We found that for ^{4}He concentrations between 2% and 34%, the ^{3}He T_c increases by a very small amount. However, ρ_s, which for pure ^{3}He in aerogel at $0.5T_c$ is no more than 11%, falls by another factor of 7. This behavior (constant T_c, reduced ρ_s) is similar to that observed in granular superconducting films where the long-range order is controlled by phase coherence between adjacent grains.

PACS numbers: 67.57.-z, 67.60.-g, 61.43.Hv

1. INTRODUCTION

Unconventional (p-wave triplet) superfluid pairing was discovered in liquid ^{3}He.[1] In superconducting metals, the role of impurities is varied,[2] with non-magnetic impurities and defects having a small influence while magnetic impurities are responsible for decreasing T_c and pairing amplitude.[3] Since impurities do not exist in superfluid ^{3}He, their influence is moot but in gen-

0022-2291/98/0100-0515$15.00/0

eral surfaces (including those of porous materials) function as pairbreaking scatterers.

We start by comparing the structure of aerogel (from a simulation) to the length scales in ^{3}He. We then describe the torsion pendulum oscillators. We compare new results to the (T_c, P) study of an earlier sample of aerogel, and discuss measurements that map out the phase diagram at very low temperatures. Lastly, we describe measurements in progress on phase separated mixtures. These phenomena point to the strong influence of aerogel on superfluid ^{3}He and the role of aerogel as the analog of an impurity that introduces disorder into the superfluid.

2. RESULTS

2.1. Simulations of the Structure of Aerogel

The structure of aerogels can be simulated using a model that mimics diffusion limited aggregation of the silica spheres.[4] These results imply that in 98.2% open aerogel, all points in the helium are within 300Å of the silica, and that the mean distance is on the order of 100Å. The geometric mean free path of a quasiparticle is found to be 2000Å for aerogel of porosity, ϕ =0.982 and scales with the porosity as $(1-\phi)^{-1.24}$. The correlations of the silica in the aerogel are set by the kinetics of the gelation process so microscopically different aerogels can be made with the same density.[5] It is possible that the reaction rates may have been different for each sample, producing slightly different correlations of silica and this factor may account for the differing results of our three samples.

To illustrate the "openness" and structure of the aerogels we show a "3D" stereoscopic rendition of 98.2% void aerogel in Fig. 1. This structure, together with a low density (39.4 g/l) and large surface area (22.9m^2/cm^3) characterize the aerogel. The zero temperature coherence length for bulk ^{3}He, $\xi_0 = \hbar v_F/2\pi k_B T_c$, ranges from 150Å at 29 bar to 800Å at saturated vapor pressure.[6] At all pressures for this density of aerogel, the Cooper pairs must encompass some silica and as the pressure is lowered, each pair must sample more silica. At any pressure, the usual boundary condition of the order parameter being brought to zero within ξ_0 of a diffusely scattering surface would lead to absence of superfluidity of ^{3}He in aerogel;[7] thus, the usual boundary condition cannot be valid at the surface of the silica.

To summarize, the aerogel's structure is radically different from that of other porous media, because of the low density and also because the silica particles are smaller than a coherence length. The size of the smallest units (30Å), the proximity of the entire volume to silica and the relatively long mean free path make aerogel a unique environment in which to study ^{3}He.

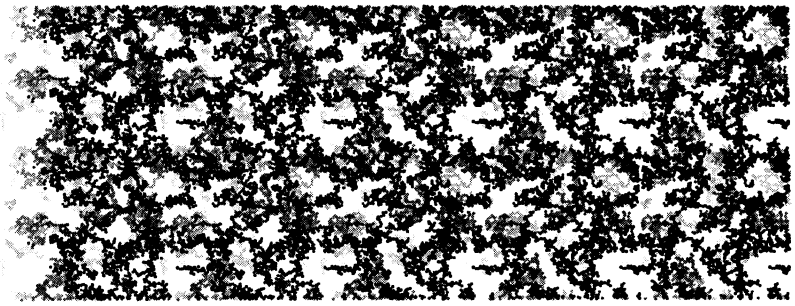

Fig. 1. A 3D stereoscopic image of a computer generated aerogel. To view the image, hold the page close to your face and defocus your eyes. Then slowly move the page 30-50 cm away from you. The dark spots should stand out and the grey ones recede from the surface.

2.2. Description of the Torsional Oscillators

For all the experiments, the aerogel was grown directly into a metal cup which was then epoxied into a mating form with an integral tube through which helium was admitted (see the inset to Fig. 3). The tube functioned as the torsion spring for the mechanical oscillator. Ideally, the cup containing the aerogel should have been pressed into its mate to avoid a planar gap which was not eliminated in the two newer cells, (B, C), resulting in a small bulk signal contribution.

A capacitor was included in cell C for mixture experiments to determine the ^{4}He content of the mixture in the aerogel. By measuring the period of the oscillator just above the bulk ^{3}He T_c and the ^{4}He content of the aerogel, χ_4, the fraction of ^{4}He coupled to the pendulum could be computed. χ_4 is directly related to the tortuosity, α, by $\alpha = 1/(1 - \chi_4)$.

We monitored the period of the oscillator which is a direct measure of the moment of inertia of the fluid coupled to the cell. Since the spacing between strands was much smaller than the viscous penetration depth, all of the normal fluid was entrained. The superfluid density was computed by measuring the decrease in the period (corresponding to a reduced moment of inertia) below the onset of superfluidity.

2.3. The phase diagram of ^{3}He in 98.2% Aerogel

There are several unique features connected with the superfluidity of ^{3}He in aerogel. T_c is well defined (better than 1%) and the transition is narrower than that observed by Freeman and Richardson[8] in a parallel plate geometry with a 3% size distribution. Above 5 bar, $d(\rho_s/\rho)/dT$ at different pressures is nearly identical close to T_c (shown in Fig. 7 and 8 of Ref. 9).

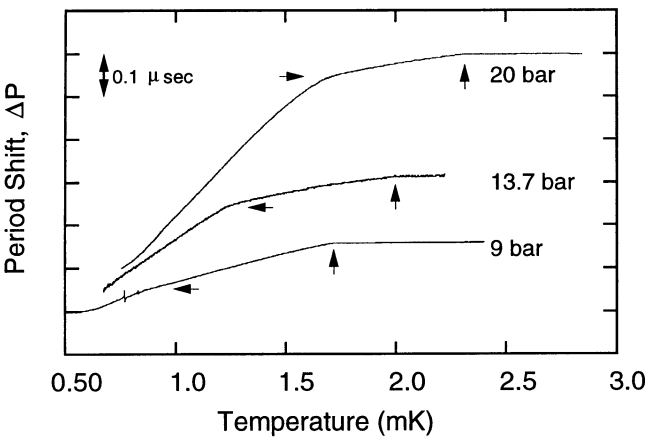

Fig. 2. Period vs T for cell B at three pressures. Horizontal arrows show T_c in aerogel. Vertical arrows show the bulk T_c. The period signal from ^{3}He in aerogel becomes much smaller than the bulk contribution at low pressures.

Slightly different power laws for ρ_s/ρ above and below 15 bar may be an indication of a phase transition – for example from an A-like to a B-like phase. However, the existence of such a phase transition is impossible to ascertain from ρ_s/ρ measurements alone. The results of Cell A have been discussed previously[9,10]and show the smallest suppression of T_c relative to the bulk.

The period vs temperature is shown in Fig. 2 for cell B. Because ρ_s in the aerogel is <1 at high pressure and decreases at lower pressures, the period shift at low pressures becomes very small and is difficult to track below 8 bar for constant-pressure temperature-sweeps, so we changed the pressure at a constant temperature while ensuring that heating was negligible. Starting from low pressure, all of the ^{3}He added to the cell contributed to the moment of inertia until a critical density,ρ_c, was exceeded. Above ρ_c the period of the pendulum fell below that of rigid body rotation and aside from a small region of rounding, we found that 90% of the fluid added above ρ_c did not contribute to the moment of inertia. This data is shown in Fig. 3. A similar plot for cell A shows that the period decreases below that at the critical density implying that a fraction of the helium below ρ_c must participate in superflow for cell A, in contrast to the results for cell B. At low temperatures, the superfluid fraction of the mass added above the critical density approaches unity.

The phase diagram for ^{3}He in aerogel (T_c vs P_c) is shown in Fig. 4. In the inset, we show a plot of ρ_c vs T_c for cells A and B, as well as the bulk fluid. It can be seen by extrapolation from the data in the inset that at zero temperature, there is a transition between two ground states, one being a

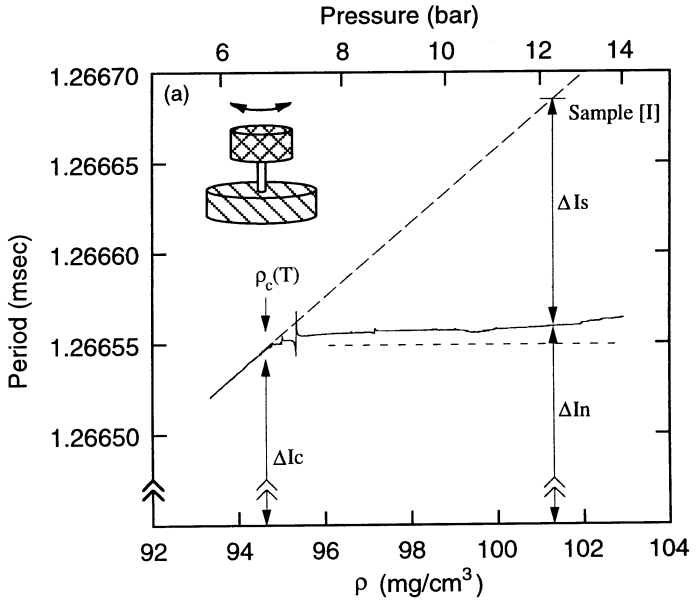

Fig. 3. Period vs density at 0.295 mK, obtained by sweeping the pressure while holding a constant temperature for five days. The critical density is indicated by an arrow. The diagonal dashed line indicates rigid body behavior of the pendulum. The inset shows a schematic picture of the cell, with the cross hatched portion representing the head (filled with aerogel) and the diagonal lines representing the silver sinter heat exchanger.

low density non-superfluid state, and the second a superfluid state. This is a quantum phase transition (QPT) and is distinguished from other transitions because it occurs between two zero entropy states, and in which quantum rather than thermal fluctuations dominate. In this case a continuous transition at $T = 0$ is induced by tuning the density of the fluid.

The existence and nature of a QPT can be determined from the critical exponents. Unfortunately, the interference of the sound modes and temperature resolution do not allow us test for scaling. The exponent for T_c vs $(\rho - \rho_c)^x$ is found to be 0.42 ± 0.04, while that for ρ_s vs $(\rho - \rho_c)^y$ is found to be 1.24 ± 0.18. These allow us to fit for ν, the dynamical scaling exponent, which we find to be 0.8 in agreement with the quantum Harris criterion.[11]

The transition temperatures for cell C are not as well defined, but if we plot T_c of aerogel samples A, B, and C vs ρ, we find that sample A most likely does not display a QPT, while B and C are closer to one another. It is likely that sample A does not behave in the same way as samples B and C which undergo QPTs, and also show that nearly all $\rho > \rho_c$ is in the

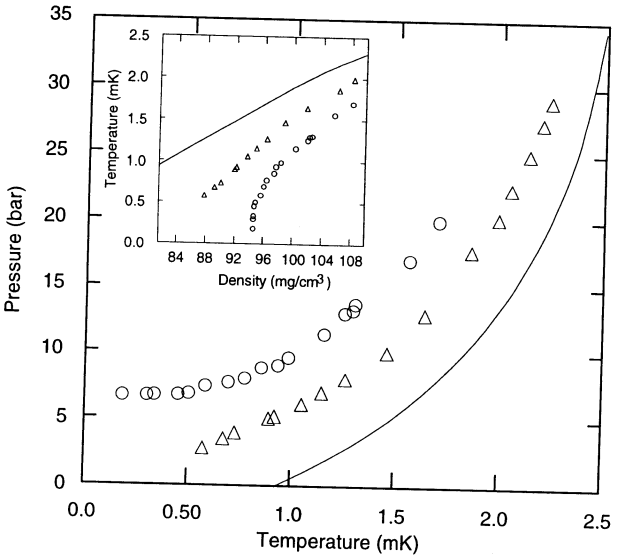

Fig. 4. Phase diagram of ^{3}He in aerogel for different cells: triangles - Cell A, circles - Cell B. The solid line shows the bulk superfluid transition. In the inset we show the same data points for T_c vs ρ_c. The existence of the QPT can be inferred by extrapolating the data in the inset to T=0. The character of the low density phase has yet to be determined.

superfluid state. The mass below critical density acts as if the Cooper pairs (if any exist at this pressure) are localized by the disorder induced by the aerogel.

2.4. Experiments on Mixtures of ^{3}He and ^{4}He

We set out to explore the behavior of the phase separated mixtures of the two isotopes at very low temperatures, following the results of the Penn State Group.[12,13] The experiments are still in progress and we have investigated three areas: i) How the addition of ^{4}He affects T_c? ii) How the presence of ^{4}He affects ρ_s? iii) Why the history of how the ^{4}He is added affects the distribution of the ^{4}He-rich phase in the aerogel?

We have observed but not shown here that the largest shift in T_c occurs when the localized layers of ^{3}He are replaced by ^{4}He. There is also an accompanying increase in ρ_s for this coverage. This effect is similar to that seen by Sprague *et al.*[14] using NMR.

In Fig. 5 we show the period shift of the pendulum with 2% ^{4}He to 34% ^{4}He in the aerogel. The periods are shifted so that they coincide at the bulk

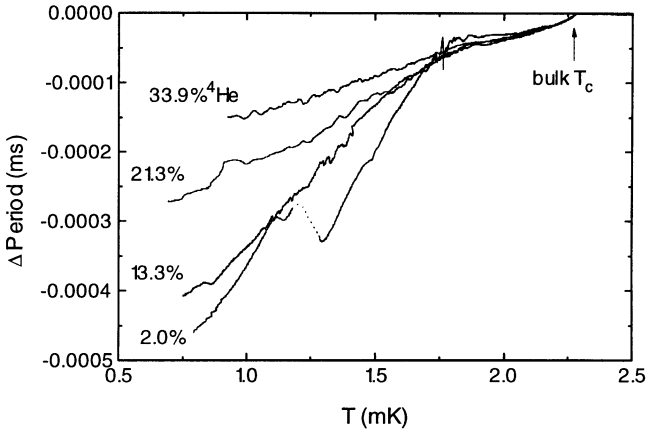

Fig. 5. Period shift with different amounts of ^{4}He added to ^{3}He at 21.6 bar. The periods have been adjusted so that they coincide at the bulk T_c. With 2% ^{4}He, ρ_s at 0.5 $T_{c-aerogel}$ is about 12%.

^{3}He transition. T_c is only weakly affected by the addition of ^{4}He, while ρ_s is strongly suppressed.

In general, the ^{4}He-rich phase preferentially fills the regions of highly correlated silica (smallest pores) first. Thus the remaining volume that the ^{3}He-rich phase occupies consists of larger voids, with relatively smooth walls. It is possible that for high ^{4}He content, phase coherence between the ^{3}He in these larger pores will weaken and the long-range-order (or superflow) can be extinguished in this limit, accounting for the decrease of the superfluid fraction with additional ^{4}He.

The particular shape of the interface between the ^{3}He- and ^{4}He-rich phases can take on any of several different metastable configurations which can be altered depending on the specific deposition conditions. For example, samples with similar ^{4}He content can give very different period shifts depending on whether the sample is deposited by initially adding pure ^{4}He or whether phase separation is achieved by cooling the mixture of ^{3}He-^{4}He from above 1K. If the ^{3}He was added while $T < 100$ mK, after the ^{4}He was deposited at low temperature, the result was a high χ_4. However, χ_4 decreased if the cell were cycled above and then cooled through the phase-separation transition, implying that deposition of ^{4}He from the homogeneous mixture improves the connections between silica strands. The data in Fig. 5 are for phase separated samples "grown" from the homogeneous mixture. The details of the ^{3}He-^{4}He phase separation will be discussed in another paper at this conference. The important point from the perspective of the superfluidity of the ^{3}He component is the fact that the presence of the ^{4}He

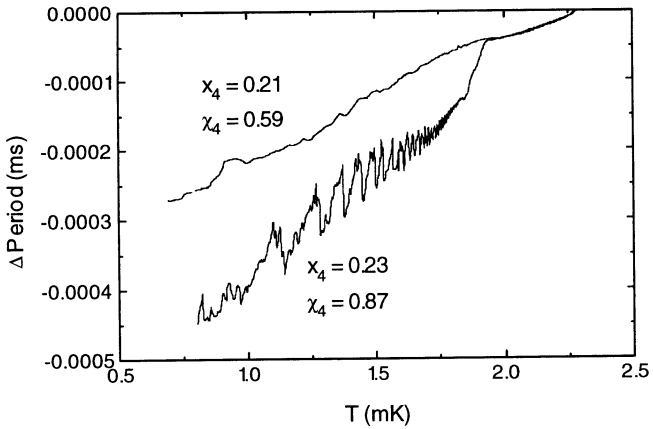

Fig. 6. Period shift for a "cold deposited" mixture sample, showing novel resonances. Also shown is the period obtained for a sample with a similar ^{4}He content but with a very different χ_4.

phase alters the distribution of the correlations of the aerogel sampled by the superfluid ^{3}He since the smallest length scales in the silica are screened by the ^{4}He-rich phase. The role of the ^{4}He depends to some extent on the sample history.

We show a plot of a data set (Fig. 6) obtained from a sample deposited at $T < 100$ mK. T_c is unaffected, but there are a series of high Q resonances that sweep through the oscillator frequency as the cell is warmed. The spacing between these resonances becomes closer (in temperature) as T_c is approached from below. These resonances may originate because of an oscillation of the ^{3}He-^{4}He interface (similar to third sound in ^{4}He) close to the substrate. The mode damping and velocity may be affected by the superfluidity of the ^{3}He "blanket". The second possibility is that the ^{3}He dissolved in a thick ^{4}He film would be induced into the superfluid state by the proximity effect. In Fig. 6 we compare the results to those obtained for a sample with nearly the same ^{4}He content but with a very different χ_4.

The small T_c shift and reduction of ρ_s with ^{4}He allow us to reject healing length effects in the aerogel, and suggests that the ^{3}He approaches the percolation threshold (at least when appreciable amounts of ^{4}He are added). Superconducting granular films show evidence of a similar phenomenon. As the connectivity of grains is altered, the experiments show that $T_c \sim T_{c-bulk}$ while the conductivity crosses over from superconducting to insulating.[15] Such a Josephson coupled system should show extraordinary sensitivity to critical currents, but signal to noise and heating effects preclude such an investigation by us at present.

3. CONCLUSIONS

The suppression of the superfluidity of ^{3}He by aerogel varies with the density of the liquid. The three cells show differences in the degree of suppression of T_c, which we hypothesize are due to the different correlations of silica in these aerogels. Depending on the sample, the $T = 0$ phase diagram exhibits a normal to superfluid transition - a quantum phase transition. The transition temperature is sharp, and ρ_s/ρ scales differently with T/T_c than in bulk ^{3}He.

Mixtures in aerogel display some fascinating behavior, with the possibility of superfluidity being induced in the ^{3}He component within the ^{4}He as well as providing clues for the nature and origin of the behavior of pure ^{3}He superfluidity in aerogel.

We would like to acknowledge the support of the National Science Foundation under DMR-9424137, the Cornell Materials Science Center, theoretical support and help from Dietrich Einzel, conversations and result sharing from Bill Halperin and Don Sprague as well as John Reppy and John Hook at Manchester. We are indebted to Moses Chan and Norbert Mulders for sample preparation.

REFERENCES

1. D. D. Osheroff, R. C. Richardson, and D. M. Lee, *Phys. Rev. Lett.* **28**, 885 (1972).
2. P. W. Anderson, *J. Phys. Chem. Sol.* **11**, 26 (1959).
3. A. A. Abrikosov and L. P. Gorkov, *Zh. Eksp. Teor. Fiz.* **12**, 1781 (1960), [*JETP*, **12**, 1243 (1961)].
4. A. Hasmy *et al. Phys. Rev.* B **50**, 6006 (1994).
5. E. Courtens *et al.*, *Phys. Rev. Lett.* **58**, 128 (1987).
6. D. S. Greywall, *Phys. Rev.* B **33**, 7520 (1986).
7. V. Ambegaokar, P. G. de Gennes and D. Rainer, *Phys. Rev.* A **9**, 2676 (1974).
8. M. R. Freeman and R. C. Richardson, *Phys. Rev.* B **41**, 11011 (1990).
9. J. V. Porto and J. M. Parpia, *Czech. J. of Phys.* **46 S-6**, 2981 (1996).
10. J. V. Porto and J. M. Parpia, *Phys. Rev. Lett.* **74**, 4667 (1995).
11. A. B. Harris, *J. Phys. C* **7**, 1671 (1974).
12. S. B. Kim, J. Ma, and M. H. W. Chan, *Phys. Rev. Lett.* **71**, 2268 (1993).
13. N. Mulders and M. H. W. Chan, *Phys. Rev. Lett.* **75**, 3705 (1995).
14. D. T. Sprague *et al.*, *Phys Rev. Lett.* **77**, 4568 (1996).
15. R. C. Dynes, R. P. Barber, and F. Sharifi, *AIP Conf. Proc.* **286**, 96, V. Srivastava, A. K. Bhatnagar, and D. G. Naugle eds., New York (1984).